PHYSICAL REVIEW D **96,** 124006 (2017)

Black-hole head-on collisions in higher dimensions

William G. Cook,[1,*] Ulrich Sperhake,[1,2,3,†] Emanuele Berti,[3,4,‡] and Vitor Cardoso[4,5,§]

[1]*Department of Applied Mathematics and Theoretical Physics, Centre for Mathematical Sciences, University of Cambridge, Wilberforce Road, Cambridge CB3 0WA, United Kingdom*
[2]*TAPIR 350-17, California Institute of Technology, 1200 E California Boulevard, Pasadena, California 91125, USA*
[3]*Department of Physics and Astronomy, University of Mississippi, University, Mississippi 38677, USA*
[4]*CENTRA, Departamento de Física, Instituto Superior Técnico, Universidade de Lisboa, Avenida Rovisco Pais 1, 1049 Lisboa, Portugal*
[5]*Perimeter Institute for Theoretical Physics, Waterloo, Ontario N2L 2Y5, Canada*

(Received 29 September 2017; published 6 December 2017)

The collision of black holes and the emission of gravitational radiation in higher-dimensional spacetimes are of interest in various research areas, including the gauge-gravity duality, the TeV gravity scenarios evoked for the explanation of the hierarchy problem, and the large-dimensionality limit of general relativity. We present numerical simulations of head-on collisions of nonspinning, unequal-mass black holes starting from rest in general relativity with $4 \leq D \leq 10$ spacetime dimensions. We compare the energy and linear momentum radiated in gravitational waves with perturbative predictions in the extreme mass ratio limit, demonstrating the strength and limitations of black-hole perturbation theory in this context.

DOI: 10.1103/PhysRevD.96.124006

I. INTRODUCTION

The study of higher-dimensional spacetimes dates back at least one hundred years to the seminal attempts by Kaluza and Klein to unify gravitation and electromagnetism. Higher dimensional arenas would resurface several times over the next decades, either in the context of specific physical theories, such as string theory, or theories which can be embedded into it. One particularly intriguing example is the class of TeV-scale gravity theories, which propose to lower the fundamental Planck scale by diluting gravity in a large number of dimensions [1,1–5]. These proposals suggest that dynamical processes involving higher-dimensional black holes (BHs) may be relevant for understanding the physics under experimental scrutiny at particle colliders, such as the Large Hadron Collider (LHC). In these scenarios, BH production would become possible at much lower energies than the four-dimensional Planck scale 10^{19} GeV, a possibility that remains interesting despite the robust constraints at current LHC energies [6,7]. In this framework, the understanding of BH dynamics and gravitational radiation emitted during high-energy encounters is fundamental [8].

Higher-dimensional spacetimes have also been used as a purely mathematical construct, where the number D of spacetime dimensions is regarded as just one other parameter to be varied. Emparan and collaborators [9–12] have recently added an elegant twist to this aspect of higher-dimensional spacetimes by focusing on the large-D limit. They showed that the physics of four-dimensional spacetimes can be recovered to good precision from a large-D expansion, and that the large-D limit offers precious physical insight into the nature of classical and quantum gravity in arbitrary dimensions.

The purpose of this work is to extend previous results on the low-energy collision of BHs to higher dimensions. This effort was started a few years ago [13,14], but a combination of gauge issues and difficulties in the regularization of variables in the dimensional reduction generated numerical instabilities, restricting all binary BH simulations to $D \leq 6$ spacetime dimensions. Building on earlier work [15,16] on the so-called *modified cartoon method*, Refs. [17,18] reported considerable progress in overcoming stability limitations and in the numerical extraction of gravitational waves (GWs) in higher-dimensional spacetimes. Using the methods developed therein, we present new results for the collision of unequal-mass BH binaries in $D = 4, 5, \ldots, 10$ dimensions, and compare these with perturbative predictions. We expect our results to also allow for making contact with the large-D regime studied by Emparan and collaborators.

II. MODELING FRAMEWORK

The physical scenario we consider in this work consists of two D-dimensional, nonspinning BHs with masses M_1 and $M_2 \leq M_1$ initially at rest, which then collide head-on under their gravitational attraction and merge into a single BH. The gravitational radiation released during the encounter of the two BHs, and its total energy and momentum in particular, is the key diagnostic quantity we wish to extract

*wc259@cam.ac.uk
†u.sperhake@damtp.cam.ac.uk
‡eberti@olemiss.edu
§vitor.cardoso@ist.utl.pt

from our calculations. For this purpose, we employ two techniques: (i) a perturbative point-particle (PP) approximation, and (ii) numerical relativity simulations assuming $SO(D-3)$ isometry. In this section we review these two methods in turn.

A. Point-particle calculations

The first attempt at understanding this process considers a somewhat restricted parameter space: one of the BHs is much more massive than the other, i.e. $q \equiv M_2/M_1 \ll 1$ or

$$\eta \equiv \frac{M_1 M_2}{(M_1+M_2)^2} = \frac{q}{(1+q)^2} \ll 1, \tag{1}$$

where η is the symmetric mass ratio. The smaller, lighter BH is then approximated as a structureless PP, moving on a geodesic of the background spacetime described by the massive BH, while generating a stress-energy tensor which perturbs it. This scheme is also sometimes known as the PP approximation. In such a framework, the resulting equations to solve are just linearized versions of the Einstein equations, expanded around a BH-background spacetime [19–24]. When the massive BH is nonspinning, the equations reduce to a single ordinary differential equation sourced by the smaller BH (the PP). In this scheme, to leading order, the total energy $E_{\rm rad} \propto q^2$. The exact coefficient was computed in Refs. [21,23,24] for particles falling radially into the BH.

Table I summarizes those results for different spacetime dimensions. Note that the proportionality coefficient increases with spacetime dimension at large D. An extrapolation of these results suggests that the perturbative PP calculation should cease to be valid at sufficiently large D, since the radiation ultimately becomes too large and the geodesic approximation breaks down: cf. the discussion around Fig. 1 of [24]. Thus, even within the PP approximation, we identify the need to solve the full, nonlinear Einstein equations at large D.

B. Numerical framework

The only presently known method to solve the Einstein equations in the dynamic and fully nonlinear regime is to use numerical tools on supercomputers: see e.g. [25–27]. In higher dimensions, however, the computational cost increases rapidly with D. To achieve sufficient resolution of all relevant scales, typical grid sizes in our simulations have $\mathcal{O}(10^2)$ grid points in each dimension, hence the computational cost increases approximately by this factor for each increment in D, making it impractical to consider arbitrary $D-1$ dimensional spatial grids. Many physical scenarios of current interest, however, involve degrees of symmetry in the extra dimensions that facilitate a reduction of the effective computational domain to three or fewer spatial dimensions, as handled in traditional numerical relativity. The physical effects of the extra dimensions are then encapsulated in a set of additional fields on the effective domain. Several approaches to achieve such a dimensional reduction have been implemented in the literature: see e.g. [15,28–30]. Here, we use the modified cartoon method in the form detailed in [17], which describes a D-dimensional spacetime with $SO(D-3)$ isometry.

TABLE I. Energy radiated in GWs when a small BH of mass qM_1, $q \ll 1$ falls from rest at infinity into a D-dimensional BH of mass M_1.

D	4	5	6	7	8
$\frac{E_{\rm rad}}{q^2 M}$	0.0104	0.0165	0.0202	0.0231	0.0292

Specifically, we use the LEAN code [31,32], originally developed for BH simulations in $D=4$ dimensions and upgraded to general D spacetime dimension with $SO(D-3)$ isometry in [17,28]. We start our simulations with the D dimensional generalization of Brill-Lindquist [33] data in Cartesian coordinates X^I (Capital Latin indices $I, J, \ldots$ cover the range $1, \ldots, D-1$, while lower case Latin indices $i, j, \ldots$ cover the range 1, 2, 3),

$$\gamma_{IJ} = \psi^{4/(D-3)}\delta_{IJ}, \qquad K_{IJ} = 0,$$
$$\psi = 1 + \sum_{\mathcal{N}} \frac{\mu_{\mathcal{N}}}{4[\sum_K (X^K - X^K_{\mathcal{N}})^2]^{(D-3)/2}}, \tag{2}$$

where γ_{IJ} and K_{IJ} are the spatial metric and extrinsic curvature of the Arnowitt-Deser-Misner (ADM) [34] formalism and we set $G = c = 1$. The index $\mathcal{N}$ labels the individual BHs and, in our case, always extends over the range $\mathcal{N} = 1, 2$. These data are evolved in time with the Baumgarte-Shapiro-Shibata-Nakamura [35,36] formulation of the Einstein equations, combined with the moving puncture [37,38] gauge and Berger-Oliger mesh refinement provided by CARPET [39,40] as part of the CACTUS computational toolkit [41,42]. In order to calculate the GW signal, we compute the higher-dimensional Weyl scalars, as detailed in [18,43,44]. For comparison and to determine the contributions of the individual multipoles, we also extract waveforms calculated with the perturbative Kodama-Ishibashi approach [22,45] as detailed in [46].

Compared with previous simulations of BH collisions in higher dimensions, we have implemented two changes we find necessary to achieve accurate and stable evolutions. First, we evolve the lapse function α according to

$$\partial_t \alpha = \beta^i \partial_i \alpha - c_1 \alpha K^{c_2}, \tag{3}$$

where β^i is the shift vector and K the trace of the extrinsic curvature; the slicing condition typically used in moving puncture simulations is recovered for $c_1 = 2$, $c_2 = 1$—cf. Eq. (11) in [31]—but here we vary these parameters in the ranges $2 \le c_1 \le 10$ and $1 \le c_2 \le 1.5$. The exact values

vary from configuration to configuration and have been determined empirically. The second modification is an approximately linear reduction of the Courant factor $\Delta t/\Delta x$ as a function of D from 0.5 in $D = 4$ to 0.03 in $D = 10$. We shall see in Fig. 2 and its discussion in Sec. III B that the merger becomes an increasingly instantaneous event with an ever sharper burst in radiation as we increase D. We believe the necessity of reducing the Courant factor to arise from this increasing demand for time resolution around merger.

III. RESULTS

In Schwarzschild coordinates, a nonrotating D-dimensional BH with ADM mass M has a horizon or Schwarzschild radius given by

$$R_S^{D-3} = \frac{16\pi M}{(D-2)\mathcal{A}_{D-2}}, \tag{4}$$

where $\mathcal{A}_{D-2} = 2\pi^{(D-1)/2}/\Gamma(\frac{D-1}{2})$. Note that R_S is related to the mass parameter μ of the single BH version of Eq. (2) by $\mu = R_S^{D-3}$. In consequence of Eq. (4), mass and length do not have the same physical dimensions unless $D = 4$. Henceforth, we measure energy in units of the ADM mass M of the spacetime under consideration, and we measure length and time in units of the Schwarzschild radius R_S associated with this ADM mass according to Eq. (4).

A. Numerical uncertainties

Our numerical relativity results for the GW energy released in head-on collisions of BHs are affected by the following uncertainties:

Discretization error.—We estimate the error due to finite grid resolution by studying a head-on collision of two BHs in $D = 8$ dimensions with mass ratio $q = 1/20$. We use a computational grid composed of 8 nested refinement levels, 2 inner boxes initially centered on the individual holes, and 6 outer levels centered on the origin. The grid spacing around the BHs is $h_1 = R_S/113$, $h_2 = R_S/129$ and $h_3 = R_S/145$, respectively, in our three simulations for checking convergence, and increases by a factor 2 on each consecutive outer level. The radiated energy as a function of time is extracted at 40 R_S, where the grid resolution is $H_i = 32h_i$ for the three runs $i = 1, 2, 3$. The difference between the high and medium resolution runs is compared with that between the medium and coarse resolution runs in Fig. 1. Multiplying the former by a factor $Q_4 = 1.88$ (as expected for the fourth-order discretization of the code) yields good agreement between the two curves, and using the according Richardson-extrapolated result gives an error estimate of 3% for the medium resolution simulation, which is closest to our set of production runs in terms of resolution around the smaller BH and in the wave extraction zone.

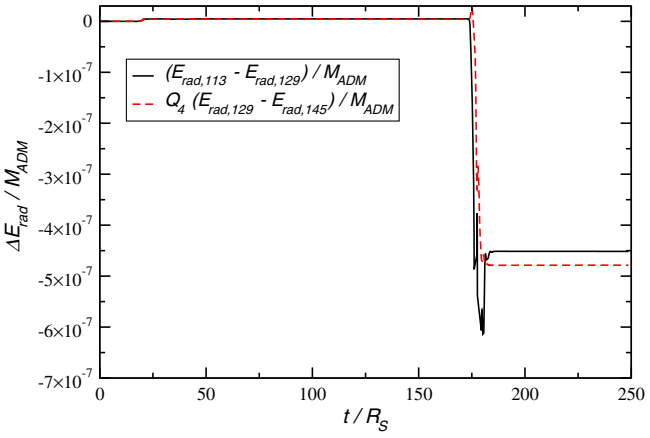

FIG. 1. Convergence plot for the radiated energy $E_{\rm rad}$ extracted from a $q = 1/20$ head-on collision in $D = 8$ at 40 R_S as a function of time for grid spacing $h_1 = R_S/113$, $h_2 = R_S/129$ and $h_3 = R_S/145$. The difference between the high and medium resolution simulations has been scaled by a factor $Q_4 = 1.88$ expected for fourth-order convergence and agrees well with the difference of the coarse and medium resolution energies.

We have analyzed several other configurations (including the collision in $D = 10$ dimensions) and find the discretization error to mildly increase with mass ratio and dimensionality D, from about 1% for $q = 1$, $D = 5$, 6 to about 4% for $q = 1$, $D = 10$ and about 5% for $q \ll 1$, $D = 8$.

Finite extraction radius.—The computational domain used in our simulations is of finite extent, about 200 R_S for the runs analyzed here, so that we cannot extract the GW signal at infinity. Instead we use finite radii and estimate the uncertainty incurred through this process by fitting the total radiated energy using a polynomial in $1/r_{\rm ex}$,

$$E_{\rm rad}(r_{\rm ex}) = E_{\rm rad} + \frac{a}{r_{\rm ex}} + \mathcal{O}\left(\frac{1}{r_{\rm ex}^2}\right), \tag{5}$$

where a is a parameter determined through fitting and $E_{\rm rad}$ is the estimate for the radiated energy extracted at infinity. We then take the extrapolated value at infinity as our result, and its difference from the largest numerical extraction radius as the uncertainty estimate. Applying this procedure yields a fractional error ranging from about 0.4% for all equal-mass collisions to about 4% for configurations with $q \ll 1$.

Spurious waves.—Initial data of the type used here typically contain a small amount of unphysical GWs colloquially referred to as "junk radiation". The amount of unphysical radiation depends on the initial separation of the BHs (vanishing in the limit of infinite distance) and on the number of dimensions. As in Ref. [18], we find the amount of spurious radiation to be orders of magnitude below the errors due to discretization and extraction radius. We attribute this to the rapid falloff of gravity in higher

dimensions, so that the constituent BHs of the Brill-Lindquist data are almost in isolation even for relatively small coordinate separations. We have noticed, however, that spurious radiation is more prominent in the Kodama-Ishibashi modes as compared with the results based on the Weyl scalars. We cannot account for the precise causes for the seemingly superior behavior of the Weyl scalars, but we note that similar findings have been reported for the $D = 4$ case in [47].

Initial separation.—The head-on collisions performed here start from finite initial separation of the BHs, while the idealized scenario considers two BHs falling in from infinity. By varying the initial separation for several collisions in $D = 5$ and $D = 6$ we estimated the difference in $E_{\rm rad}$ due to the initial separation and, as for the junk radiation above, we found that the differences are well below the numerical error budget. Again, we attribute this observation to the rapid falloff of the gravitational attraction for large D, leading to a prolonged but nearly stationary infall phase followed by an almost instantaneous merger that generates nearly all of the radiation. In summary, our error is dominated by discretization and use of finite extraction radii. It ranges from about 1.5% for comparable mass collisions in low D to about 9% for $q \ll 1$ in $D = 8$. For the gravitational recoil, we find similar significance of the individual error contributions, but overall larger uncertainties by about a factor of 4. We attribute these larger uncertainties to the fact that the recoil arises from asymmetries in GW emission, and in this sense it is a weaker, differential effect.

B. Equal-mass collisions

The collision of two equal-mass BHs has already been studied in $D = 4$, 5 [13], and $D = 6$ [14] spacetime dimensions. We have verified those results, extending them to $D = 7$, 8, 9, 10. For illustration, in Fig. 2 we plot a normalized energy flux $(R_S/M)\dot{E}$ for collisions in $D = 4$, 6, 8 and 10 spacetime dimensions. As D increases, the burst of radiation becomes increasingly concentrated in time. This concentration suggests that the burst may approach a δ distribution in the large-D limit; it would be interesting to see if this is borne out in the large-D limit formalism of [9–12].

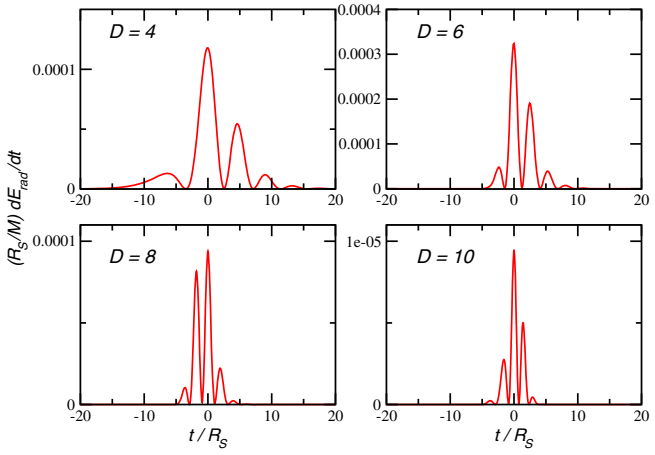

FIG. 2. Normalized energy flux $(R_S/M)\dot{E}_{\rm rad}$ as a function of time for equal-mass collisions, with $t = 0$ defined by the maximum in $\dot{E}_{\rm rad}$. As D increases, the burst of radiation becomes increasingly concentrated in time.

For further illustration, in Fig. 3 we plot the Kodama-Ishibashi waveform $\dot{\Phi}_{l0}$ [14,22,45,46] for $D = 10$; the qualitative features of the signal are the same for all other D. The waveform consists of a precursor part with small amplitude when the two BHs are widely separated, followed by a smooth merger phase connecting to ringdown. A perturbative calculation, using direct integration techniques, yields the following two modes for gravitational-type scalar perturbations: $\omega R_S = 1.2346 - 0.9329i$ and $\omega R_S = 2.4564 - 0.9879i$. These are the decoupling (or saturating) and nondecoupling (or nonsaturating) modes in the language of Refs. [48,49] (Ref. [50]). We find agreement to the level of ~0.1% or better with Ref. [50] and very good agreement with the analytical, large-D estimates of Ref. [48]. A one-mode fit of numerical waveforms yields very poor agreement with any of the frequencies above. However, a two-mode fit yields the following two frequencies: $\omega R_S = 2.48 - 0.94i$, $1.22 - 0.91i$. Given the errors in numerical simulations, this is a reasonable level of agreement with linearized predictions, and it indicates that both modes are excited to comparable amplitudes for this particular simulation.

When plotted as a function of the number D of dimensions (Fig. 4), the fraction of center-of-mass energy radiated in GWs by equal-mass head-on collisions reaches a maximum $E_{\rm rad}/M \sim 9.1 \times 10^{-4}$ for $D = 5$. Beyond this value, we find the total radiation output to rapidly decrease as a function of D. This suppression is consistent with the fact that the spacetime is nearly flat outside the horizon: in

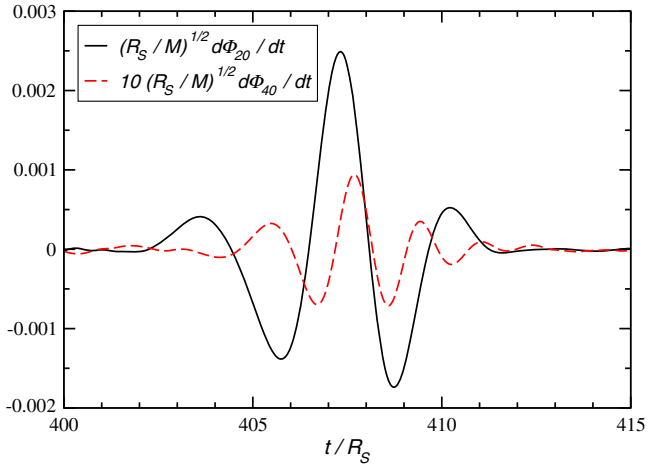

FIG. 3. The $l = 2$ (solid black line) and $l = 4$ (dashed red line) waveforms from the collision of two equal-mass BHs in $D = 10$.

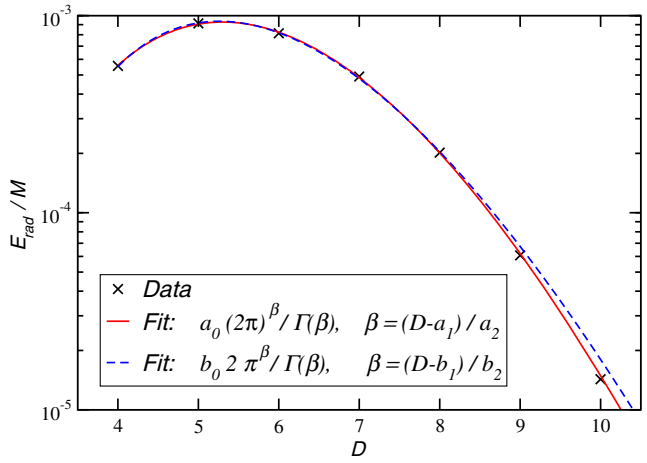

FIG. 4. Fractional energy $E_{\rm rad}/M$ radiated in GWs during collisions of equal-mass, nonspinning BHs starting from rest, in D spacetime dimensions. Crosses are numerical data points and the solid red line is the fit (6). The blue dashed line shows a fit obtained for the expression $b_0 2\pi^\beta/\Gamma(\beta)$ which resembles even more closely the functional form of the surface area $A_{D-2} = 2\pi^{(D-1)/2}/\Gamma[(D-1)/2]$ of the $D-2$ sphere, but does not match the data points as well.

fact, the gravitational potential $(R_S/r)^{D-3}$ vanishes exponentially with D [9]. Another intuitive explanation for this rapid decay is that, as D increases, the energy is radiated almost instantaneously (cf. Fig. 2): spacetime is flat except extremely near the horizons, and bremsstrahlung radiation is suppressed. These features have also been seen in zero-frequency limit calculations [51]. Thus, at large D, radiation is emitted in a burst precisely when the BHs collide, but this is also the instant where one would expect common horizon formation, and consequent absorption of a sizable fraction of this energy. This is, of course, a very loose description, unable to give us a quantitative estimate. The results in Fig. 4 are (perhaps surprisingly) well described by the following simple analytic expression,

$$\frac{E_{\rm rad}^{q=1}}{M} = a_0 \frac{(2\pi)^\beta}{\Gamma[\beta]}, \qquad \beta = \frac{D-a_1}{a_2}, \tag{6}$$

where $a_0 = 1.7288\times 10^{-6}$, $a_1 = 1.5771$, $a_2 = 0.5497$. This fit reproduces our numerical results to within $\sim 1\%$ for all $D = 4,\ldots,10$. It is tempting to relate this expression to the area $A_{D-2} = \frac{2\pi^{(D-1)/2}}{\Gamma(\frac{D-1}{2})}$ of a $(D-2)$-dimensional unit sphere, but we do not see an evident connection as the numerical factors do not match exactly.[1]

[1]The expression $b_0 2\pi^\beta/\Gamma(\beta)$ resembles even more closely that of the surface area A_{D-2}, but yields a less accurate fit to the data points (cf. Fig. 4). It also does not establish a satisfactory relation between A_{D-2} and the numerical parameters appearing in the fit for β, now given by $\beta = (D-2.4772)/0.7671$.

The results for the radiated energy are in stark contrast to the predictions one would get by applying the PP results of Table I to the equal-mass case $q=1$, where, instead of a strong suppression of $E_{\rm rad}$ at large D, we see a mild increase in the radiative efficiency. While the PP approximation is by construction not expected to capture the equal-mass limit with high precision, it is valuable to understand the origin of this qualitative discrepancy. A tantalizing suggestion in this context was made by Emparan and collaborators [9], who pointed out that—for large D—BH spacetimes contain two scales $\mathcal{L}$ of interest for BH physics. One scale can be parametrized by the areal radius $\mathcal{L}\sim R_S$ of the horizon. The other scale, absent at low D, is related to the strong localization of the gravitational potential close to the horizon: $\mathcal{L}\sim R_S/D$. For equal-mass collisions the excitation of the latter modes (and the radiation output) are strongly suppressed at large D [9]. However, dynamical processes are very sensitive to the dominant scale in higher dimensions [9,51]. In the next section, we explore in more detail unequal-mass collisions and indeed find that these collisions can trigger the excitation of smaller-scale modes even at the low energies considered in our simulations.

C. Unequal-mass collisions and the point-particle limit

The stark contrast between the PP results summarized in Table I and the numerical relativity calculations of the previous section strongly points towards a qualitatively different behavior of the radiated energy as a function of D for comparable-mass binaries (where $E_{\rm rad}$ rapidly drops beyond $D=6$) as compared with the high mass-ratio regime (where $E_{\rm rad}$ mildly increases with D). The question we are now facing is: does the difference in the behavior arise from the dominance of different physical mechanisms in the respective regions of the parameter space, and where does the crossover from one regime to the other occur? To shed light on this issue, we have performed collisions of unequal-mass, nonspinning BHs focusing on the range $q=1,\ldots,1/100$ and $D=4,\ldots,8$. The GW energy and linear momentum radiated in these collisions are summarized in Figs. 5–7.

By analyzing the waveforms for the most extreme mass ratios we find good agreement between the ringdown stage and estimates from linearized perturbations. However, our results indicate that only the high-frequency modes (the "nonsaturating" modes) are excited. Since these modes probe the small scales presumably excited by the smaller BH [10,12], it is reassuring to find high-frequency excitations.

Figure 5 shows the fractional center-of-mass energy released as GWs when two BHs collide, with and without normalization by (the square of) the kinematic, symmetric mass ratio parameter η. Note that η is directly connected to the reduced mass of the system and is known to yield a very good rescaling of all quantities in four-dimensional spacetimes (see for instance Refs. [52–54]). For low D

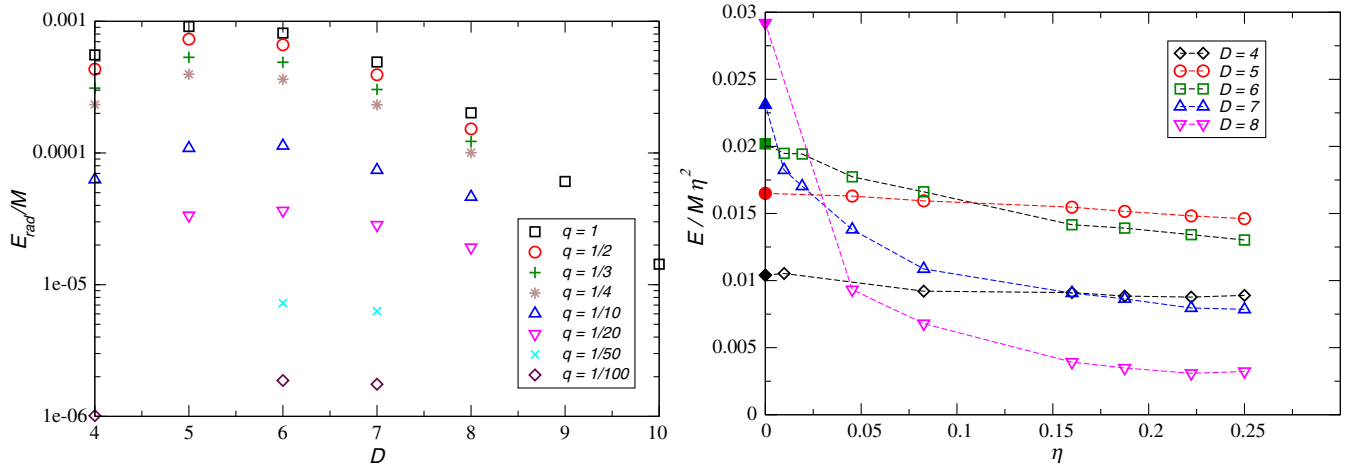

FIG. 5. Left panel: fractional energy $E_{\rm rad}/M_{\rm ADM}$ radiated in GWs in collisions of nonspinning BHs starting from rest with mass ratio q in D spacetime dimensions. Right panel: same data as in the left panel, but rescaled by η^2 [i.e. we plot $E_{\rm rad}/(M\eta^2)$] in order to facilitate the comparison with PP calculations of the radiated energy, which are shown as filled symbols at $\eta = 0$.

(in particular for $D = 4$, 5) the total radiated energy $E_{\rm rad}/(M\eta^2)$ is weakly dependent on η. At small mass ratios q, or equivalently at small η, our results smoothly approach the PP limit of Table I (shown in Fig. 5 as filled data points at $\eta = 0$).

For $q \lesssim 1$ and sufficiently large D, the radiated energy decreases monotonically with D (left panel of Fig. 5). This behavior would clearly contradict the PP results if it held for arbitrarily small mass ratio. In fact, at small mass ratios the behavior of the radiated energy changes. The maximum of the radiated energy as a function of D shifts from $D = 5$ to $D = 6$ between $q = 1/4$ and $q = 1/10$. Results for even smaller q indicate a further shift towards $D = 7$, and possibly yet higher D as we approach the PP limit. Furthermore, we see from the right panel of Fig. 5 that $E_{\rm rad}/(M\eta^2)$ shows a steep increase for very small η and large D. This behavior supports our interpretation that new scales are being probed. If this is indeed the correct interpretation, and if the new scale is of order R_S/D, one can estimate the mass ratio at which these new scales are excited. By using Eq. (4), and recalling that $M_2/M_1 = q$, we get the scaling $(r_2/R_S)^{D-3} = q$, with r_2 the scale of the small BH and R_S the scale of the large BH in terms of coordinate quantities. If we equate the "small scale" R_S/D to the size r_2 of the second colliding object we find the threshold mass ratio

$$q \sim D^{3-D}. \tag{7}$$

It seems sensible to understand the mass ratio dependence by *fixing* the PP limit to be that of Table I. In other words, we fit our results to the expression

$$\frac{E_{\rm rad}}{M\eta^2} = b_0 + b_1\eta^{b_2}, \tag{8}$$

where b_0 are the PP values listed in Table I. The exponents b_2 obtained by fitting our data are listed in Table II. These numbers are consistent with the behavior shown in Fig. 5: the dependence of the total radiated energy on η is more complex for large D. In particular, at large D the expansion of $E_{\rm rad}$ in powers of η converges more slowly, and the convergence of the PP results (a leading-order expansion in mass ratio) is poor in the small-η regime. It would be interesting to find an analytical prediction for the coefficient b_2.

D. Kicks

In Fig. 6, we show the gravitational recoil (or "kick") velocity of the postmerger BH as a function of D for fixed values of the mass ratios q. As in the case of the radiated energy (left panel of Fig. 5), we observe a shift in the maximum kick towards higher D as the mass ratio decreases. In particular, the maximum shifts from $D = 6$ to $D = 7$ as we change q from $1/4$ to $1/10$. In Fig. 7 we show the same results, but now plotting the kick for fixed D as a function of the symmetric mass ratio η.

The data in Figs. 6 and 7 are in good agreement with PP recoil calculations [24,55,56]: for example, in $D = 4$ the PP calculation yields $P_{\rm rad}/M = 8.33 \times 10^{-4}q^2$, or $v_{\rm kick} = 250q^2$ km/s. This is in percent-level agreement with the $D = 4$, $\eta = 0.01$ simulation, for which we get $v_{\rm kick} = 0.026$ km/s (for such small mass ratios, of course,

TABLE II. Fitting coefficients of Eq. (8), describing the η dependence of the total radiated energy.

D	4	5	6	7	8
$-10^2 b_1$	0.54	0.95	2.82	3.63	3.58
b_2	0.72	1.18	0.83	0.44	0.19

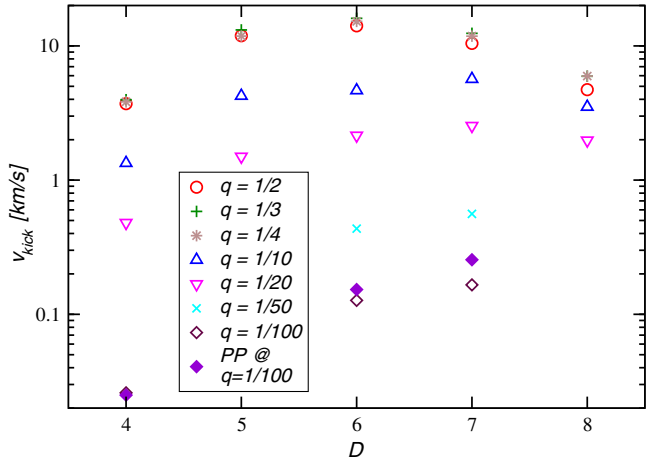

FIG. 6. Recoil due to asymmetric emission of GWs in the collision of nonspinning BHs starting from rest with mass ratio q in D spacetime dimensions. Note that the agreement with PP predictions in the small-q limit is very good for $D = 4$, and degrades for higher D.

$q \simeq \eta = 0.01$). As D increases, the PP prediction becomes less accurate: the relative error is 4% in $D = 4$, 21% in $D = 6$ and 54% in $D = 7$. This is consistent with the trend observed for the radiated energy and with physical expectations: according to Eq. (4), for a fixed q the less massive black hole appears less and less like a PP. It is also possible that some of this disagreement comes form the larger errors in the high-D, small-mass ratio simulations.

Following previous work on unequal mass collisions in $D = 4$ dimensions [57] we first tried to fit the data using the following mass ratio dependence (see e.g. the classic work by Fitchett and Detweiler [58]):

$$v^{(1)}_{\rm kick} = v_D \eta^2 \sqrt{1-4\eta}, \tag{9}$$

where the superscript (1) means that this is a one-parameter fit. According to this simple formula, the maximum recoil occurs when $\eta = 0.2$ ($q \simeq 0.38$) for all D. Note that for $\eta = 0.2$ we get $v^{(1)}_{\rm kick,max} \simeq 0.018 v_D$, so the parameter v_D is related to the maximum kick by a simple proportionality relation.

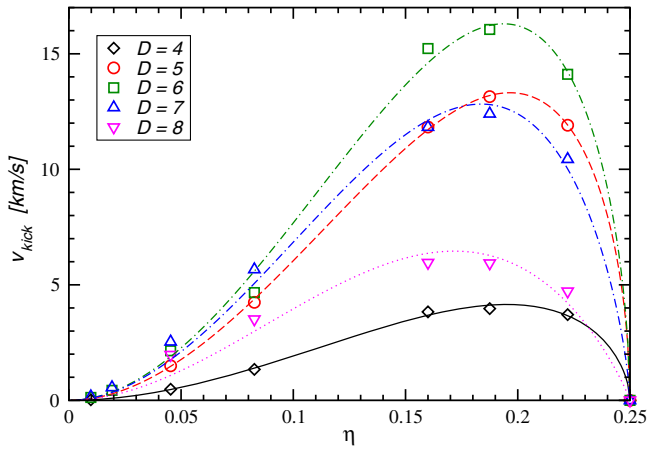

FIG. 7. As Fig. 6 but here symbols denote the kick for fixed D as a function of the symmetric mass ratio η. The lines are the simple two-parameter fit of Eq. (10).

TABLE III. Fitting coefficients of Eqs. (9) and (10), describing the η dependence of the kick velocity.

D	4	5	6	7	8
v_D[km/s]	232.9	746.9	915.2	714.8	349.0
$v^{(1)}_{\rm kick,max}$[km/s]	4.166	13.361	16.372	12.787	6.244
$\tilde{v}_D$[km/s]	255.8	798.4	1034	989.9	630.7
c_D	0.5629	0.5445	0.5821	0.7214	0.9110
$\eta_{\rm max}$	0.1951	0.1965	0.1936	0.1837	0.1718
$v^{(2)}_{\rm kick,max}$[km/s]	4.148	13.314	16.297	12.822	6.457

However, our previous considerations suggest that the mass ratio dependence of the radiated energy and of the recoil velocity should vary with D. As a simple way to investigate this D dependence we used a two-parameter fitting function:

$$v^{(2)}_{\rm kick} = \tilde{v}_D \eta^2 (1-4\eta)^{c_D}. \tag{10}$$

Assuming this dependence, the maximum kick $v^{(2)}_{\rm kick,max}$ will correspond to a D-dependent $\eta_{\rm max}$ that can be obtained by fitting the data.

The fitting coefficients and maximum kicks obtained with these two expressions are listed in Table III. Note that the D dependence of $\eta_{\rm max}$ is very mild for all but the largest D simulations. More accurate simulations may be needed to resolve the issue of the D-dependence of $\eta_{\rm max}$ and of the maximum kick velocity. However, the following conclusion is quite independent of the assumed functional dependence: the maximum kick is ~16.3 km/s, and it is achieved for $D = 6$ and $\eta_{\rm max} \simeq 0.2$.

IV. CONCLUSIONS

We have numerically simulated head-on collisions of black holes in $D = 4, \ldots, 10$ dimensions, extracted the GW signal and computed the energy and linear momentum radiated in the collisions. Starting with the equal-mass case, we find values for the radiated energy in agreement with previously published results for $D = 5$ and $D = 6$ dimensions. The radiated energy, measured in units of the ADM mass M, is maximal in $D = 5$, where $E_{\rm rad}/M = 9.1 \times 10^{-4}$. For larger D we observe a strong reduction in the radiated energy: the fit $E_{\rm rad}/M = (2\pi)^\beta/\Gamma(\beta)$, $\beta = (D - 1.5771)/(0.5497)$ models our results to within 1% for all D simulated. This functional dependence closely resembles that of the surface area $\mathcal{A}_{D-2} = 2\pi^{(D-1)/2}/\Gamma[(D-1)/2]$, but the discrepancy in the numerical parameters in the argument suggests a more complicated relation between the two quantities.

The numerical results for the equal-mass case differ strikingly from those obtained in the PP approximation, which predicts a mild increase of $E_{\rm rad}/(q^2M)$ with D when a small BH of mass qM_1, $q \ll 1$ falls into a BH of mass M_1. We reconcile these seemingly different predictions by numerically simulating a wider set of BH collisions with mass ratios ranging from $q = 1$ to $q = 1/100$ in up to $D = 8$ dimensions. In the right panel of Fig. 5 we observe that the (symmetric mass ratio-normalized) energy $E_{\rm rad}/(M\eta^2)$ increases in the PP limit $q \to 0$. This increase becomes particularly steep for $D = 7$ and $D = 8$, and the numerical data extrapolated to $q = 0$ are in good agreement with the PP predictions.

These findings can be understood by invoking the presence of multiple length scales in the large-D limit, as identified in [9]: Additionally to the length scale R_S of the Schwarzschild horizon, the large-D limit reveals a shorter scale R_S/D for the spatial variation of potential terms in the equations governing BH perturbations. It is natural then to assume that these shorter length scales will be excited with much higher efficiency by a small object falling into a BH, while they are largely insensitive to the collision of two objects of size R_S. The parameter regime in between these two extremes, on the other hand, is characterized by excitations of comparable magnitude on both length scales.

Our intuitive interpretation is strengthened by the analysis of the quasinormal mode frequencies: for $q = 1$ (and large D) the ringdown exhibits comparable contributions from two frequencies, corresponding to the "saturating" and "unsaturating" modes in the language of [50], while the ringdown is dominated by the unsaturating modes for $q \ll 1$. For large D, the emission of gravitational waves therefore appears to be sensitive to the properties of the two BHs. It is interesting to contrast this observation with the corresponding *insensitivity* of the collision dynamics in high-energy collisions in $D = 4$ [59,60]. This contrast naturally raises the question which effect dominates in high-energy, large-D collisions: sensitivity to structure due to large D or universality due to high energy?

With regard to the large-D limit, we notice a further connection in the shape of the energy flux as a function of time. In units of the Schwarzschild horizon associated with the ADM mass of the spacetime, the flux becomes increasingly peaked in higher D and it appears to approach the shape of a δ distribution, which is what one would intuitively expect in the large-D limit, where the spacetime exterior to a BH approaches Minkowski.

Finally, we analyze the gravitational recoil resulting from the asymmetric emission of GWs in unequal-mass collisions. We find the data to be well fitted by Fitchett's [58] formula commonly applied to the four-dimensional case, but we also observe a mild indication that the mass ratio maximizing the recoil varies with D at large D. The maximum kick due to gravitational recoil ($v_{\rm kick,max} \sim 16.3$ km/s) is achieved for $D = 6$, and for a symmetric mass ratio $\eta = \eta_{\rm max} \simeq 0.2$ ($q \simeq 0.4$). When regarding both energy or linear momentum as a function of D at fixed mass ratio q, we observe a shift in the maximum towards higher D as we move from the equal-mass case $q = 1$ to the PP limit $q \ll 1$. This observation further confirms one of our main conclusions: the PP limit provides exquisitely accurate predictions for small mass ratios, but it must be taken with a grain of salt when extrapolated to the comparable-mass regime in higher dimensions.

ACKNOWLEDGMENTS

We are grateful to Roberto Emparan for numerous suggestions and for sharing with us some numerical results. We thank Pau Figueras, Markus Kunesch, Chris Moore, Saran Tunyasuvunakool, Helvi Witek and Miguel Zilhão for very fruitful discussions on this topic. V. C. is indebted to Kinki University in Osaka for hospitality while the last stages of this work were being completed. U.S. and V. C. acknowledge financial support provided under the European Union's H2020 ERC Consolidator Grant "Matter and strong-field gravity: New frontiers in Einstein's theory" Grant Agreement No. MaGRaTh–646597. Research at Perimeter Institute is supported by the Government of Canada through Industry Canada and by the Province of Ontario through the Ministry of Economic Development Innovation. E. B. was supported by NSF Grants No. PHY-1607130 and No. AST-1716715, and by FCT Contract No. IF/00797/2014/CP1214/CT0012 under the IF2014 Programme. This work has received funding from the European Union's Horizon 2020 research and innovation programme under the Marie Skłodowska-Curie Grant Agreement No. 690904, the COST Action Grant No. CA16104, from STFC Consolidator Grant No. ST/L000636/1, the SDSC Comet, PSC-Bridges and TACC Stampede clusters through NSF-XSEDE Award No. PHY-090003, the Cambridge High Performance Computing Service Supercomputer Darwin using Strategic Research Infrastructure Funding from the HEFCE and the STFC, and DiRAC's Cosmos Shared Memory system through BIS Grant No. ST/J005673/1 and STFC Grants No. ST/H008586/1 and No. ST/K00333X/1. W. G. C. is supported by a STFC studentship. We acknowledge PRACE for awarding us access to MareNostrum at Barcelona Supercomputing Center (BSC), Spain under Grant No. 2016163948.

[1] I. Antoniadis, A possible new dimension at a few TeV, Phys. Lett. B **246**, 377 (1990).

[2] N. Arkani-Hamed, S. Dimopoulos, and G. R. Dvali, The hierarchy problem and new dimensions at a millimeter, Phys. Lett. B **429**, 263 (1998).

[3] I. Antoniadis, N. Arkani-Hamed, S. Dimopoulos, and G. R. Dvali, New dimensions at a millimeter to a Fermi and superstrings at a TeV, Phys. Lett. B **436**, 257 (1998).

[4] L. Randall and R. Sundrum, A Large Mass Hierarchy from a Small Extra Dimension, Phys. Rev. Lett. **83**, 3370 (1999).

[5] L. Randall and R. Sundrum, An Alternative to Compactification, Phys. Rev. Lett. **83**, 4690 (1999).

[6] M. Aaboud *et al.*, Search for new phenomena in dijet events using 37 fb^{-1} of pp collision data collected at $\sqrt{s} =$ 13 TeV with the ATLAS detector, Phys. Rev. D **96**, 052004 (2017).

[7] A. M. Sirunyan *et al.*, Search for black holes in high-multiplicity final states in proton-proton collisions at sqrt(s) = 13 TeV, arXiv:1705.01403.

[8] V. Cardoso, L. Gualtieri, C. Herdeiro, and U. Sperhake, Exploring new physics frontiers through numerical relativity, Living Rev. Relativity **18**, 1 (2015).

[9] R. Emparan, R. Suzuki, and K. Tanabe, The large D limit of general relativity, J. High Energy Phys. 06 (2013) 009.

[10] R. Emparan, T. Shiromizu, R. Suzuki, K. Tanabe, and T. Tanaka, Effective theory of Black Holes in the 1/D expansion, J. High Energy Phys. 06 (2015) 159.

[11] R. Emparan, R. Suzuki, and K. Tanabe, Evolution and End Point of the Black String Instability: Large D Solution, Phys. Rev. Lett. **115**, 091102 (2015).

[12] R. Emparan and K. Tanabe, Universal quasinormal modes of large D black holes, Phys. Rev. D **89**, 064028 (2014).

[13] H. Witek, V. Cardoso, L. Gualtieri, C. Herdeiro, U. Sperhake, and M. Zilhão, Head-on collisions of unequal mass black holes in $D = 5$ dimensions, Phys. Rev. D **83**, 044017 (2011).

[14] H. Witek, H. Okawa, V. Cardoso, L. Gualtieri, C. Herdeiro, M. Shibata, U. Sperhake, and M. Zilhão, Higher dimensional numerical nelativity: Code comparison, Phys. Rev. D **90**, 084014 (2014).

[15] F. Pretorius, Numerical relativity using a generalized harmonic decomposition, Classical Quantum Gravity **22**, 425 (2005).

[16] H. Yoshino and M. Shibata, Higher-dimensional numerical relativity: Formulation and code tests, Phys. Rev. D **80**, 084025 (2009).

[17] W. G. Cook, P. Figueras, M. Kunesch, U. Sperhake, and S. Tunyasuvunakool, Dimensional reduction in numerical relativity: Modified cartoon formalism and regularization, Int. J. Mod. Phys. D **25**, 1641013 (2016).

[18] W. G. Cook and U. Sperhake, Extraction of gravitational-wave energy in higher dimensional numerical relativity using the Weyl tensor, Classical Quantum Gravity **34**, 035010 (2017).

[19] T. Regge and J. A. Wheeler, Stability of a Schwarzschild Singularity, Phys. Rev. **108**, 1063 (1957).

[20] F. J. Zerilli, Gravitational field of a particle falling in a Schwarzschild geometry analyzed in tensor harmonics, Phys. Rev. D **2**, 2141 (1970).

[21] M. Davis, R. Ruffini, W. H. Press, and R. H. Price, Gravitational radiation from a particle falling radially into a Schwarzschild black hole, Phys. Rev. Lett. **27**, 1466 (1971).

[22] H. Kodama and A. Ishibashi, A master equation for gravitational perturbations of maximally symmetric black holes in higher dimensions, Prog. Theor. Phys. **110**, 701 (2003).

[23] E. Berti, M. Cavaglia, and L. Gualtieri, Gravitational energy loss in high energy particle collisions: Ultrarelativistic plunge into a multidimensional black hole, Phys. Rev. D **69**, 124011 (2004).

[24] E. Berti, V. Cardoso, and B. Kipapa, Up to eleven: Radiation from particles with arbitrary energy falling into higher-dimensional black holes, Phys. Rev. D **83**, 084018 (2011).

[25] F. Pretorius, in *Physics of Relativistic Objects in Compact Binaries: From Birth to Coalescence*, edited by M. Colpi *et al.* (Springer, New York, 2009).

[26] J. M. Centrella, J. G. Baker, B. J. Kelly, and J. R. van Meter, Black-hole binaries, gravitational waves, and numerical relativity, Rev. Mod. Phys. **82**, 3069 (2010).

[27] U. Sperhake, The numerical relativity breakthrough for binary black holes, Classical Quantum Gravity **32**, 124011 (2015).

[28] M. Zilhão, H. Witek, U. Sperhake, V. Cardoso, L. Gualtieri, C. Herdeiro, and A. Nerozzi, Numerical relativity for D dimensional axially symmetric space-times: Formalism and code tests. Phys. Rev. D **81**, 084052 (2010).

[29] E. Sorkin, An Axisymmetric generalized harmonic evolution code, Phys. Rev. D **81**, 084062 (2010).

[30] H. Yoshino and M. Shibata, Higher-dimensional numerical relativity: Current status, Prog. Theor. Phys. Suppl. **189**, 269 (2011).

[31] U. Sperhake, Binary black-hole evolutions of excision and puncture data, Phys. Rev. D **76**, 104015 (2007).

[32] U. Sperhake, E. Berti, V. Cardoso, J. A. González, B. Brügmann, and M. Ansorg, Eccentric binary black-hole mergers: The transition from inspiral to plunge in general relativity, Phys. Rev. D **78**, 064069 (2008).

[33] D. R. Brill and R. W. Lindquist, Interaction Energy in Geometrostatics, Phys. Rev. **131**, 471 (1963).

[34] R. Arnowitt, S. Deser, and C. W. Misner, in *Gravitation an Introduction to Current Research*, edited by L. Witten (John Wiley, New York, 1962), p. 227.

[35] M. Shibata and T. Nakamura, Evolution of three-dimensional gravitational waves: Harmonic slicing case, Phys. Rev. D **52**, 5428 (1995).

[36] T. W. Baumgarte and S. L. Shapiro, On the Numerical integration of Einstein's field equations, Phys. Rev. D **59**, 024007 (1998).

[37] J. G. Baker, J. Centrella, D.-I. Choi, M. Koppitz, and J. van Meter, Gravitational-Wave Extraction from an Inspiraling Configuration of Merging Black Holes, Phys. Rev. Lett. **96**, 111102 (2006).

[38] M. Campanelli, C. O. Lousto, P. Marronetti, and Y. Zlochower, Accurate Evolutions of Orbiting Black-Hole Binaries without Excision, Phys. Rev. Lett. **96**, 111101 (2006).

[39] E. Schnetter, S. H. Hawley, and I. Hawke, Evolutions in 3-D numerical relativity using fixed mesh refinement, Classical Quantum Gravity **21**, 1465 (2004).

[40] CARPET Code, http://www.carpetcode.org/.
[41] G. Allen, T. Goodale, J. Massó, and E. Seidel, The Cactus Computational Toolkit and Using Distributed Computing to Collide Neutron Stars, in *Proceedings of Eighth IEEE International Symposium on High Performance Distributed Computing, HPDC-8, Redondo Beach, 1999* (IEEE Press, Piscataway, New Jersey, 1999).
[42] CACTUS Computational Toolkit, http://www.cactuscode.org/.
[43] M. Godazgar and H. S. Reall, Peeling of the Weyl tensor and gravitational radiation in higher dimensions, Phys. Rev. D **85**, 084021 (2012).
[44] W. G. Cook and U. Sperhake (to be published).
[45] A. Ishibashi and H. Kodama, Perturbations and stability of static black holes in higher dimensions, Prog. Theor. Phys. Suppl. **189**, 165 (2011).
[46] H. Witek, M. Zilhão, L. Gualtieri, V. Cardoso, C. Herdeiro, A. Nerozzi, and U. Sperhake, Numerical relativity for D dimensional space-times: Head-on collisions of black holes and gravitational wave extraction, Phys. Rev. D **82**, 104014 (2010).
[47] C. Reisswig, C. D. Ott, U. Sperhake, and E. Schnetter, Gravitational wave extraction in simulations of rotating stellar core collapse, Phys. Rev. D **83**, 064008 (2011).
[48] R. Emparan, R. Suzuki, and K. Tanabe, Decoupling and non-decoupling dynamics of large D black holes, J. High Energy Phys. 07 (2014) 113.
[49] R. Emparan, R. Suzuki, and K. Tanabe, Quasinormal modes of (Anti-)de Sitter black holes in the 1/D expansion, J. High Energy Phys. 04 (2015) 085.
[50] O. J. C. Dias, G. S. Hartnett, and J. E. Santos, Quasinormal modes of asymptotically flat rotating black holes, Classical Quantum Gravity **31**, 245011 (2014).
[51] V. Cardoso, O. J. C. Dias, and J. P. S. Lemos, Gravitational radiation in D-dimensional space-times, Phys. Rev. D **67**, 064026 (2003).
[52] E. Berti, V. Cardoso, J. A. González, U. Sperhake, M. D. Hannam, S. Husa, and B. Brügmann, Inspiral, merger and ringdown of unequal mass black hole binaries: A multipolar analysis, Phys. Rev. D **76**, 064034 (2007).
[53] A. Le Tiec, A. H. Mroue, L. Barack, A. Buonanno, H. P. Pfeiffer, N. Sago, and A. Taracchini, Periastron Advance in Black Hole Binaries, Phys. Rev. Lett. **107**, 141101 (2011).
[54] A. Le Tiec, The overlap of numerical relativity, perturbation theory and post-Newtonian theory in the binary black hole problem, Int. J. Mod. Phys. D **23**, 1430022 (2014).
[55] T. Nakamura and M. P. Haugan, Gravitational radiation from particles falling along the symmetry axis into a Kerr black hole: The momentum radiated, Astrophys. J. **269**, 292 (1983).
[56] E. Berti, V. Cardoso, T. Hinderer, M. Lemos, F. Pretorius, U. Sperhake, and N. Yunes, Semianalytical estimates of scattering thresholds and gravitational radiation in ultra-relativistic black hole encounters, Phys. Rev. D **81**, 104048 (2010).
[57] U. Sperhake, V. Cardoso, C. D. Ott, E. Schnetter, and H. Witek, Extreme black hole simulations: Collisions of unequal mass black holes and the point particle limit, Phys. Rev. D **84**, 084038 (2011).
[58] M. J. Fitchett and S. Detweiler, Linear momentum and gravitational waves—Circular orbits around a Schwarzschild black hole, Mon. Not. R. Astron. Soc. **211**, 933 (1984).
[59] U. Sperhake, E. Berti, V. Cardoso, and F. Pretorius, Universality, Maximum Radiation and Absorption in High-Energy Collisions of Black Holes with Spin, Phys. Rev. Lett. **111**, 041101 (2013).
[60] U. Sperhake, E. Berti, V. Cardoso, and F. Pretorius, Gravity-dominated unequal-mass black hole collisions, Phys. Rev. D **93**, 044012 (2016).